

ON THE USE OF POLARIZATION CAMERAS FOR THE DETERMINATION OF CONCRETE MOISTURE

S. Isfort*, F. Maiwald, C. Mulsow, H.-G. Maas

Institute of Photogrammetry and Remote Sensing, Technische Universität Dresden, Germany
(steffen.isfort, ferdinand.maiwald, christian.mulsow, hans-gerd.maas)@tu-dresden.de

KEY WORDS: polarimetry, polarization camera, surface moisture, 3D concrete printing, 3DCP, degree of polarization

ABSTRACT:

3D concrete printing (3DCP) promises progress in the automation of the construction industry. The complexity and high quality requirements of 3DCP require automatic and digital control processes and systems that can continuously assess quality at any time and any place. In this paper, the relationship between the surface moisture of concrete and the degree of linear polarization (DoLP) of light reflected from the concrete surface is investigated, which could serve as a basis for a camera-based control system. To proof this correlation, extensive practical investigations were carried out in which a mold-cast concrete specimen was illuminated with a white LED spotlight. The reflected light was recorded with a polarization camera, and the weight of the specimen served as a reference for the surface moisture. 14 experimental tests showed a high correlation between mass loss and DoLP with a mean correlation coefficient of 0.994 in the last 60 minutes of the 180-minute observation period. The time series show an increasing DoLP at the beginning of the observation period, which is probably due to the concrete bleeding and does not correlate with the mass loss. Further investigation into the factors influencing the DoLP in the first part of the observation period needs to be carried out, either by testing influencing factors such as concrete bleeding or by finding a reliable method to measure surface moisture to correlate it with the DoLP over the entire observation period. Nevertheless, the concept and methodology of data processing has been developed and prototyped, and a correlation has been demonstrated, that can provide a basis for the development of an operational camera-based concrete moisture monitoring system.

1. INTRODUCTION

In recent decades, many sectors such as manufacturing and agriculture have seen an increase in productivity. However, the productivity of the construction sector has increased far less. The reasons for this are seen, for example, in a lack of innovation, automation and digitalization (Barbosa et al., 2017). While there are already well-developed and adopted digital techniques such as computer aided design (CAD) and building information modelling (BIM), there is still a gap with a non-digital, manual building process that has not fundamentally changed for decades. As concrete is the most widely used building material in the world, digital fabrication technologies such as 3D concrete printing (3DCP), in combination with existing technologies such as CAD and BIM, have the potential to digitize and automate the construction process from design to fabrication. This promises various economic benefits, such as reduced construction times, improved quality and lower costs for complex structures. Besides the economic potential, better material efficiency through topology-optimized structures according to the principle "form follows force" may lead to lower material consumption and thus reduce CO₂ emissions from the construction sector (Wangler et al., 2019; de Schutter et al., 2018).

While the term 3DCP encompasses different techniques, this paper focuses on extrusion-based printing, which is most commonly used in research and industry (Mechtcherine et al., 2020). Fresh concrete is pumped to a print head and precisely placed in layers. The print head is mounted on a gantry or robot arm and is positioned by a computer controlled process which

is derived from a 3D model (Buswell et al., 2018). Extrusion-based 3DCP has already been used in several projects worldwide (PERI GmbH, 2020b; Yingchuang Building Technique Co Ltd. (WinSun), 2022; Walsh, 2019). In practice, however, this technique is not yet widespread, primarily due to the various technical challenges of the printing process. The material must meet high requirements when it passes from a fluid, extrudable stage to a solid stage while new printing layers are applied (de Schutter et al., 2018). During this process, various types of failures can occur. These are, for example, failures related to the printed shape and geometry, cracking and shrinkage, and a low interlayer bond strength of the printed layers (Hou et al., 2021). To avoid such failures and to prove that the intended design and quality have been reached, control processes and systems are required. According to (Wolfs et al., 2018a), such a system should fulfil three requirements:

1. the manufacturing process is monitored continuously
2. the acquired data is used for real-time quality control
3. a closed feedback loop reacts upon the quality control when required

Furthermore, a possible control system should correspond to the digital character of the manufacturing process.

Most control systems developed focus on the printed shape and geometry and use, for example, 3D laser scanning, photogrammetry or structured light. An overview is given by (Buswell et al., 2020). Another approach by (Wolfs et al., 2018b) continuously adjusts the print head height relative to the print surface. Our approach aims to survey the concrete moisture, which affects the interlayer bond strength of printed concrete layers. So

* Corresponding author



Figure 1. 3D concrete printer from PERI GmbH. Printable concrete is applied in layers and no formwork is required. Cameras are attached to the print head for visual monitoring of the printing process and results ©PERI GmbH (PERI GmbH, 2020a).

far, surface moisture has been measured by relatively simple methods such as placing a paper towel on the concrete and measuring the weight before and after placement (Sanjayan et al., 2018). This method is neither digital and automatic, nor continuously and real-time, it also lacks reproducibility and is therefore not suitable for a quality control system in a printing process, measured against the previously mentioned requirements. For this reason, a different approach is investigated in this paper. It is based on the properties of the reflected light, which is linearly polarized depending on the moisture content of the reflecting material (Curran, 1981; Egan et al., 1968). The reflected light is measured with a polarization camera, which allows the determination of polarization parameters such as the degree of linear polarization (DoLP). Polarization is used in various applications, such as food quality control, 3D shape retrieval and material characterization. An overview is given by (Snik et al., 2014). But so far it has not been used for measuring the moisture content of a material with a polarization camera in the close range. The purpose of this paper is to investigate whether there is a relationship between the DoLP and the surface moisture content of concrete. If so, this could be the basis for the development of a non-contact, automatic and real-time control system for the surface moisture in 3DCP. As cameras are already used in the visual control of the printing process (PERI GmbH, 2020b), a camera-based control system for surface moisture seems to be a good addition as its images can also be used for visual purposes.

The paper is structured in four sections. The following section 2 gives a brief overview of concrete surface moisture, its role in 3DCP and a method to measure. Section 3 provides an overview on the polarization of light and the way it is used to determine the surface moisture. The 4th section gives details on the experimental setup, the used polarization camera and data processing. Finally, the experimental results are presented in Section 5.

2. ON THE INFLUENCE OF SURFACE MOISTURE IN 3DCP

The interlayer bond strength is an important factor in achieving the desired mechanical properties and high durability. It is influenced by a number of factors, such as the print head speed, the print nozzle height, the material properties and the interval

time between two printed layers (Hou et al., 2021). The latter is related to the surface moisture of the previous layer, as shown in (Wolfs et al., 2019), (Keita et al., 2019) and (Sanjayan et al., 2018) by testing mechanical properties of concrete specimens of different ages and surface moisture. All show that the inter-layer bond strength increases with increasing surface moisture and vice versa, making it a parameter worth controlling. For a more comprehensive overview of research on time gap and surface moisture, see (Babafemi et al., 2021). The surface moisture is essentially influenced by concrete bleeding and evaporation. Bleeding is a process in which solids with a higher density compared to the density of water settle, while water rises to the surface. This causes the surface moisture to increase over time (Ghourchian et al., 2017). Evaporation counteracts this and depends on the relative humidity of the air, the temperatures of the air and of the surface water, as well as on wind speed and solar radiation (Uno, 1998). In addition, the printing process influences the initial surface moisture through the pressure exerted on the concrete during the pumping and extrusion process. The surface moisture is therefore dependent on the printing process and extruder type (Marchment et al., 2019).

While (Wolfs et al., 2019) and (Keita et al., 2019) investigate the influence of moisture indirectly by testing mechanical properties on specimens of different ages and comparing them with specimens of the same age covered with a plastic film to prevent evaporation, (Sanjayan et al., 2018) measure the surface moisture directly and link it to mechanical tests. For that purpose, they placed a paper towel on the surface of a concrete sample for 20 seconds. The towel absorbed the surface water, the change in weight after 20 seconds is a measure of surface moisture. With different delay times, the surface moisture was measured at least three times, for both mold-cast and printed concrete, where the specimens were the same size and had the same humidity and air temperature. Figure 2 shows the results. The surface moisture of the mold-cast concrete increased, which was probably due to the fact that the concrete bleeding exceeded evaporation. The printed concrete, on the other hand, had a higher surface moisture at the beginning, which was due to pressurized bleeding caused by the pressure exerted during printing. The surface moisture then decreased because there was no bleeding, only evaporation, and increased after 20 minutes when bleeding began. For more details, see (Sanjayan et al., 2018).

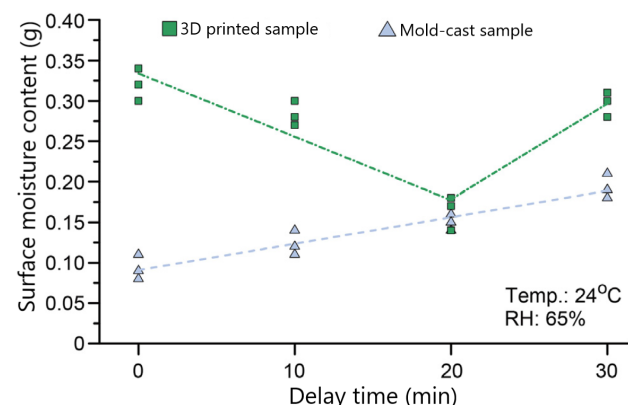


Figure 2. Surface moisture of printed and mold-cast concrete, measured by application of a paper towel (Sanjayan et al., 2018).

3. POLARIZATION OF LIGHT

Besides wavelength, frequency and amplitude, polarization is a parameter for describing the properties of an electromagnetic wave. Polarization describes the orientation of the oscillations in the plane that is perpendicular to the direction of propagation. If the direction of oscillation changes randomly with time, light is called unpolarized. In contrast, it is called linear polarized, if the orientation is constant over time (Tipler et al., 2019). Other types of polarization, such as circular or elliptical polarized light, are not relevant to this work and are therefore not considered further. The polarization state of light can be described by the four Stokes parameters. The first parameter S_0 describes the full intensity of light, the parameters S_1 , S_2 and S_3 describe the partial intensity of light in different polarization states. The polarization parameters can be easily determined by intensity measurements of light that has passed polarization filters with different filter orientations (Goldstein, 2011; Perkins and Gruev, 2010).

$$\begin{aligned} S_0 &= I_0 + I_{90} \\ S_1 &= I_0 - I_{90} \\ S_2 &= I_{45} - I_{135} \end{aligned} \quad (1)$$

The Stokes parameters allow the calculation of additional polarization parameters, such as the DoLP, which describes the proportion of light in the linear polarization state (Takruri et al., 2020).

$$DoLP = \frac{\sqrt{S_1^2 + S_2^2}}{S_0}, \quad 0 \leq DoLP \leq 1 \quad (2)$$

In general, light is unpolarized. It is polarized, for example, by absorption, scattering and birefringence. In addition, light is polarized by specular reflection. When unpolarized light hits a smooth surface such as a perfectly smooth water surface at an angle τ , it is partially specularly reflected at the angle τ and partially transmitted through the material. The reflected part of the light is partially or completely polarized by the reflection. The degree of polarization depends on the angle of incidence τ and the refractive indices of the materials forming the boundary layer (Tipler et al., 2019). In contrast, light can be assumed to be unpolarized when it is diffuse reflected from rough surfaces. Incident light is reflected more than once on microfacets of the rough surface or inside the material surface. The specific reflection differs for each light wave, thus also the degree and direction of polarization. Diffusely reflected light is therefore considered as a sum of light waves with different reflection paths, which leads to different polarization properties, similar to unpolarized light (Wolff, 1990).

The measurement principle is now based on the difference in polarization due to reflection from specular and diffuse surfaces. A water-saturated concrete surface is assumed to behave similar like a smooth water surface, thus reflected light is linearly polarized by specular reflection. An unsaturated concrete surface is dominated by diffuse reflection from the rough concrete surface, the reflected light is unpolarized. It follows that the degree of linear polarization of reflected light should be larger with higher moisture content of the concrete surface. The correlation has already been investigated and demonstrated experimentally in the moisture determination of soils by reflected visible light (Curran, 1981; Egan et al., 1968).

4. POLARIZATION CAMERA AND EXPERIMENTAL SETUP

As already mentioned, the polarization properties of light reflected from the concrete surface are to be measured. For that purpose, the polarization camera Mako G 508-B from Allied Vision was used for the practical experiments.¹ Its monochromatic CMOS sensor IMX250MZR from Sony has a size of 2464 x 2056 pixels and a radiometric resolution of 8 to 12 bits. The camera is powered and controlled via an Ethernet connection and has a C-mount for lenses. The construction of the camera follows the division of focal plane scheme by placing a polarization filter in front of each sensor pixel. Four different filter orientations (0° , 45° , 90° , 135°) are deposited in a group of four pixels called a superpixel (figures 3, 4). In this way, each superpixel allows the calculation of the first three Stokes parameters and the degree of linear polarization according to the equations (1) and (2), respectively. Since the four pixels of a superpixel have different instantaneous fields of view, the four sub-sampled images containing only one polarization channel must be interpolated to the full sensor resolution to avoid errors in the computed polarization information, similar to the interpolation in Bayer-pattern RGB images. Through the interpolation, all four polarization filter information is available for each pixel and the polarization parameters can be calculated for each pixel. Here, bicubic interpolation was used to interpolate all four sub-sampled images, as it shows good results for the division of focal plane polarization sensors (Gao and Gruev, 2011). The polarization camera was controlled by a self-written C++ routine, based on the Vimba C++ API provided by the camera manufacturer.² Images were automatically acquired

¹ <https://www.alliedvision.com/en/camera-selector/detail/mako/g-508b-pol/> (accessed 23 February 2022)

² <https://www.alliedvision.com/en/products/vimba-sdk/> (accessed on 23 February 2022)

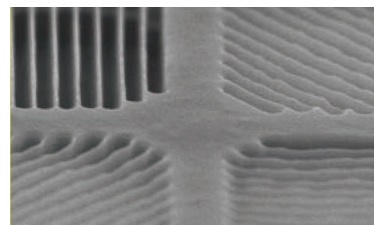


Figure 3. Photograph of the polarization camera's wire grid, © Sony Corporation Copyright 2016 (Yamazaki et al., 2016).

90	45	90	45
135	0	135	0
90	45	90	45
135	0	135	0

Figure 4. Polarization coding of physical pixel array, © Allied Vision Technologies GmbH Copyright 2021.

at defined time intervals and the four sub-images were interpolated using bicubic interpolation implemented by OpenCV³. This makes it possible to obtain all necessary information for determining pixelwise linear polarization parameters in a single image in real-time, which makes the approach particularly useful for kinematic applications such as 3DCP.

A series of practical experiments was performed to proof the correlation between the surface moisture of concrete and the degree of linear polarization. For this purpose, a concrete specimen was illuminated with a white LED spotlight and the reflected light was recorded with a polarization camera on the opposite side, both aligned at the same angle according to the law of refraction (figure 5). For each of the 14 tests, a concrete specimen was produced and placed between the spotlight and the camera. During a period of 180 minutes, images were taken every 2 minutes, the specimen was weighed on a precision balance every 5 minutes and the relative humidity and air temperature were recorded. The Stokes parameters and the degree of polarization were calculated for each pixel. For all pixels of the concrete specimen, the average degree of linear polarization was calculated as an arithmetic value, resulting in an average degree of linear polarization for the specimen in each shot.

The specimen was formed manually with a spatula, since the initial purpose of this work is to demonstrate the relationship between the DoLP and the moisture content of any concrete surface. While printing a concrete specimen requires a lot of concrete, the manually formed specimen saves resources as only the required amount of concrete is mixed. All specimens consisted of a non-printable mixture of water, cement type CEM I 42,5 R and sand with a grain size of ≤ 2 mm. All ingredients were weighed and mixed, and the water was at the same temperature as the ambient air. All weighing was done with a precision balance, and the concrete mixes of all specimens followed the same recipe. The specimen was formed in a wooden mould, which was sealed with epoxy. The specimen had a size of about 15 x 15 cm and was only a few millimetres thick in order to minimize the influence of concrete bleeding and thus make the course of concrete surface moisture dependent only on evaporation, which was captured by weighing. Since evaporation depends on the humidity and temperature of the surrounding atmosphere, both were measured at regular intervals to analyse their influence on the surface moisture and the DoLP.

³ <https://opencv.org/> (accessed on 23 February 2022)

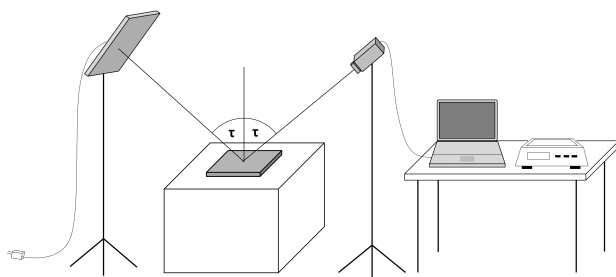


Figure 5. Experimental setup. A white LED spotlight illuminated a concrete specimen, the reflected light was captured with a polarization camera. The specimen was weighed in regular intervals, the camera was automatized to capture and interpolate polarized images.

Test Nr.	Correlation Coefficient
1	0,987
2	0,987
3	0,988
4	0,998
5	0,991
6	0,997
7	0,994
8	0,995
9	0,999
10	0,997
11	0,993
12	0,999
13	0,994
14	0,996

Table 1. Correlation coefficients between the mean DoLP time series and the linearized weight time series for each test in the last 60 minutes with a mean correlation coefficient of 0.994 for all tests.

5. RESULTS

Figure 6 shows the mean DoLP time series for each test carried out, figure 7 shows the time series for the weight of the specimens. All DoLP time series are almost noise-free, as they show the mean value over several pixels. This basically qualifies the approach, especially for dynamic applications with time-varying parameters and kinematic measurements. At the beginning, all DoLP time series show an increase, which theoretically corresponds to an increased surface moisture. After 30-40 minutes, most DoLP time series reach a maximum and start to decrease approximately linearly. At the same time, an approximately linear decrease in specimen weight is measured in all experiments. It is likely that the increase in DoLP in the first 30-40 minutes is caused by the concrete bleeding, although attempts were made to minimize its influence by making a thin specimen. The bleeding overshadows the evaporation at the beginning, similar to the results of (Sanjayan et al., 2018) for mold-cast concrete (figure 2). Surface moisture and DoLP increase until bleeding decreases and stops and evaporation is the only influencing factor for surface moisture.

5.1 Correlation between probe weight and DoLP

In the further course of the experiment, the results show a very high correlation between the specimen's mean DoLP time series and its weight time series. Since the measured values of DoLP and weight were not equidistant, a linear model function for the weight was calculated and used to calculate the weight values in the two-minute interval like the DoLP values. The modelled weight values were correlated with the DoLP values. For the last 60 minutes of the observation period, the mean correlation coefficient of all tests is 0.994. Table 1 shows the correlation coefficients for all tests. This period was chosen because evaporation is probably the only influencing factor for the surface moisture measured by weighing. Further research is needed to proof the correlation between DoLP and surface moisture for the entire observation period, also including the rise at the beginning. For example, by measuring the bleeding rate (Josserand and de Larrard, 2004) to investigate its influence at the beginning, or by theoretically modelling the course of the surface moisture. Nevertheless, the correlation shown is a strong indication of the usefulness of the DoLP as a parameter to measure concrete surface moisture. This is also in agreement with the findings of (Sanjayan et al., 2018).

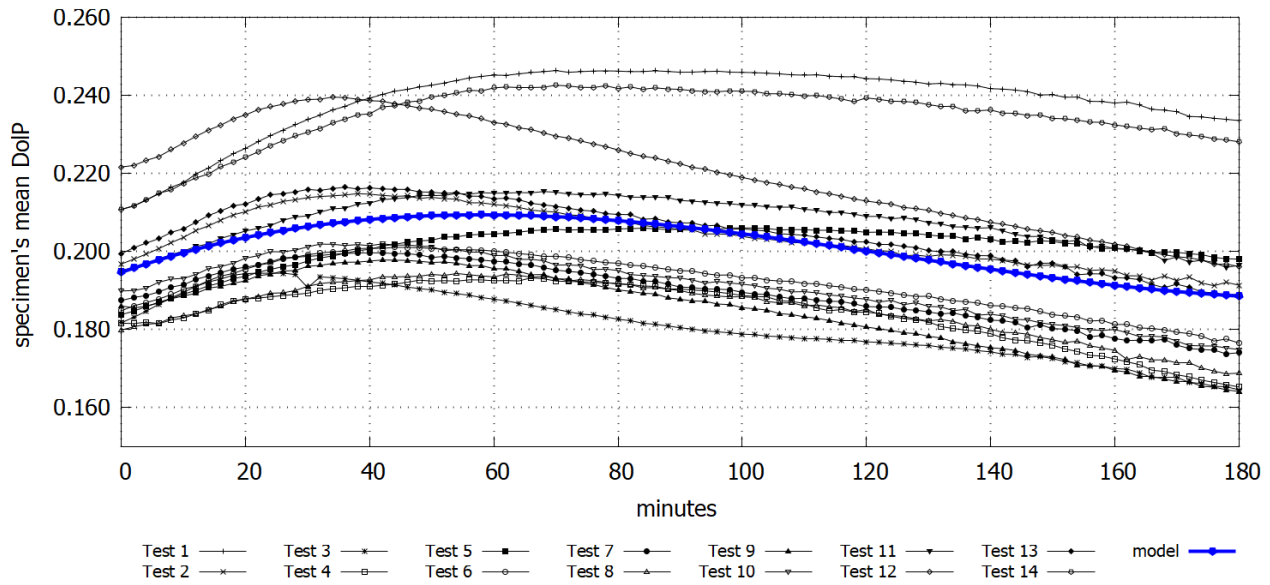


Figure 6. Time course of the mean degree of linear polarization of 14 concrete specimens during 180 minutes.

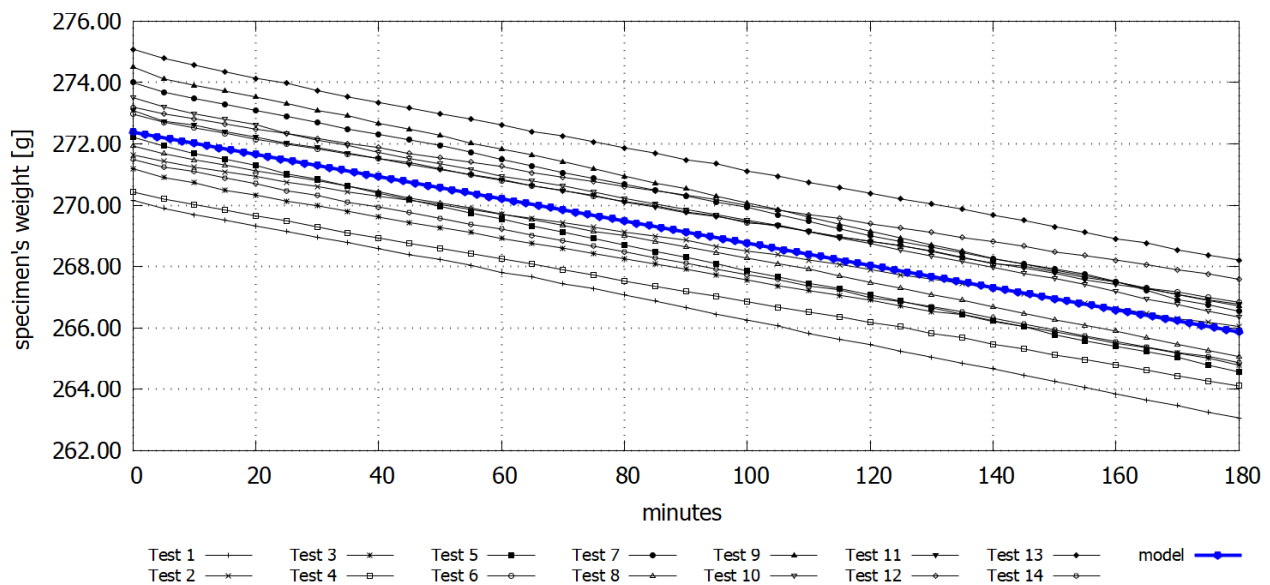


Figure 7. Time course of the weight loss due to evaporation of 14 concrete specimens during 180 minutes. The weight loss has been used as reference for the concrete surface moisture.

5.2 Variation between experiments

Besides the correlation, an analysis of the variations between the 14 time series was also carried out. The variations in the initial weight were caused by small differences in the amount of mixed concrete used during the moulding process, for example small concrete residues in the mixing cup and on the spatula. The initial specimen weight varies in a range of about 5 grams, which is less than 2 percent of the total weight of the specimens. The variations in the mean DolP time series are probably also due to the moulding process. The pressure exerted on the specimen during moulding has an influence on the water distribution, comparable to the influence of the printing process (Section 2). In order to ensure that factors such as relative humidity, air temperature and variations in specimens weight do not have an influence, a statistical analysis was carried out. Therefore, model

functions were calculated for the time series of the mean DolP as well as for the time series of the weight, which are shown in figures 6 and 7.

The model functions were calculated using multiple linear regression, with the regression coefficients estimated using the least squares method (Niemeier, 2008). The model function for mean DolP follows the equation 3, where the only influencing variable t is time. The model function for weight follows equation 4, influencing variables are relative humidity (RH), air temperature (T) and time (t).

$$DolP_i = b_0 + t_i b_1 + t_i^2 b_2 + t_i^3 b_3 \quad (3)$$

$$weight_i = b_0 + RH_i b_1 + T_i b_2 + t_i b_3 \quad (4)$$

where:

$$DolP_i/weight_i = \text{observation } i$$

$$b_n = \text{regression coefficient } n$$

$$t_i = \text{time of observation } i$$

$$RH_i = \text{relative humidity of observation } i$$

$$T_i = \text{temperature of observation } i$$

All influence variables were tested and proven to be significant. The coefficient of determination is 0.99998 for the weight model and 0.99147 for the mean DolP model. The weight function was calculated using the mean temperature and mean relative humidity of all tests throughout the observation period, which are 26.2°C and 47.0%, respectively. Then the difference of each time series from its model function was calculated. Then each difference series of the DolP and the weight was correlated pairwise. It can be seen that the correlations are widely scattered and not systematic. Therefore, the variations of the specimens weight have no influence on the variations of the mean DolP series. Since the weight model function depends on the air temperature and relative humidity, both have no influence on the mean DolP series. The main influencing factor on the mean DolP variations is therefore probably the pressure exerted during manual moulding, which is not exactly repeatable. The pressure has an influence on the initial surface moisture and the initial water distribution and thus influences the surface moisture during the observation period.

5.3 Spatial variation

The DolP was determined as the mean value for the entire specimen. Besides noise reduction, this was also motivated by movements of the specimen, which prevents a simple mapping of equal pixels over time. Furthermore, weighing the specimen as documentation of evaporation and as a reference measurement for surface moisture does not allow the determination of pixel-wise reference values, but only for the entire specimen. Figure 8 shows the DolP value for each specimen pixel of a test at the start time. It shows a large scatter of DolP values reaching from zero polarization to a maximum DolP of about 0.7 with a mean DolP of 0.203 and a standard deviation of 0.069. The distribution is not uniform, especially the pixels in the lower part of the specimen show high DolP values. This irregular distribution of the DolP can be observed throughout the observation period. It is probably due to the manual moulding process mentioned in the previous section, where pressure is applied with the spatula, resulting in an irregular moisture distribution. Another reason is probably the inhomogeneous material and thus reflection properties. Since concrete is not a homogeneous material, reflection can occur on different materials such as sand and cement with different reflection and polarization properties.

6. CONCLUSION

In this study we investigated whether the surface moisture of concrete can be determined with the help of a polarization camera. For this purpose, a concept was developed and prototypically implemented in which the surface moisture is determined from the partial images of the four polarization channels via the Stokes parameters, which describe the linear polarization state. The correlation between the surface moisture and the degree of polarisation was investigated in extensive practical experiments. The functionality of the implemented algorithms for

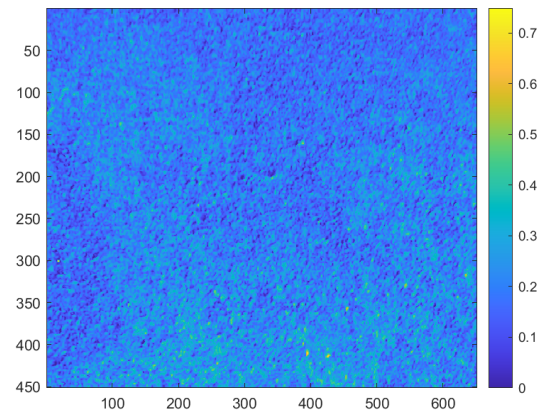


Figure 8. Degree of linear polarization at starting time, right after forming the specimen.

data acquisition, interpolation and processing could be demonstrated, which enable real-time data processing. A high correlation between the linear degree of polarization of the reflected light and the surface moisture of the concrete is shown with an average correlation coefficient of 0.994 in the last 60 minutes of a 180-minute observation period in all experiments. The results can serve as a basis for the development of a system for automatic and continuous real-time monitoring of the surface moisture in 3D concrete printing. In order to obtain physically meaningful results, a material physics model must be developed to link the measured degree of linear polarization and the surface moisture and to deliver a quantitative linear moisture parameter. In addition, the results can be considered as a basis for further investigations in the field of moisture measurement in the close range by means of polarization properties.

References

- Babafemi, A. J., Kolawole, J. T., Miah, M. J., Paul, S. C., Panda, B., 2021. A Concise Review on Interlayer Bond Strength in 3D Concrete Printing. *Sustainability*, 13(13), 7137.
- Barbosa, F., Woetzel, J., Mischke, J., Ribeirinho, M. J., Sridhar, M., Parsons, M., Bertram, N., Brown, S., 2017. Reinventing construction through a productivity revolution. <https://www.mckinsey.com/business-functions/operations/our-insights/reinventing-construction-through-a-productivity-revolution> (accessed 16 February 2022).
- Buswell, R. A., Leal de Silva, W. R., Jones, S. Z., Dirrenberger, J., 2018. 3D printing using concrete extrusion: A roadmap for research. *Cement and Concrete Research*, 112, 37–49.
- Buswell, R., Kinnell, P., Xu, J., Hack, N., Kloft, H., Maboudi, M., Gerke, M., Massin, P., Grasser, G., Wolfs, R., Bos, F., 2020. Inspection methods for 3d concrete printing. F. P. Bos, S. S. Lucas, R. J. Wolfs, T. A. Salet (eds), *Second RILEM International Conference on Concrete and Digital Fabrication*, RILEM Bookseries, 28, Springer International Publishing, Cham, 790–803.
- Curran, P. J., 1981. Remote sensing: the use of polarized visible light (PVL) to estimate surface soil moisture. *Applied Geography*, 1(1), 41–53.

- de Schutter, G., Lesage, K., Mechtcherine, V., Nerella, V. N., Habert, G., Agusti-Juan, I., 2018. Vision of 3D printing with concrete — Technical, economic and environmental potentials. *Cement and Concrete Research*, 112, 25–36.
- Egan, W. G., Grusauskas, J., Hallock, H. B., 1968. Optical depolarization properties of surfaces illuminated by coherent light. *Applied optics*, 7(8), 1529–1534.
- Gao, S., Gruev, V., 2011. Bilinear and bicubic interpolation methods for division of focal plane polarimeters. *Optics express*, 19(27), 26161–26173.
- Ghouchian, S., Wyrzykowski, M., Lura, P., 2017. A practical approach for reducing the risk of plastic shrinkage cracking of concrete. *RILEM Technical Letters*, 2, 40–44.
- Goldstein, D. H., 2011. *Polarized Light*. 3. edn, CRC Press, Boca Raton, Fla.
- Hou, S., Duan, Z., Xiao, J., Ye, J., 2021. A review of 3D printed concrete: Performance requirements, testing measurements and mix design. *Construction and Building Materials*, 273, 121745.
- Josserand, L., de Larrard, F., 2004. A method for concrete bleeding measurement. *Materials and Structures*, 37(10), 666–670.
- Keita, E., Bessaies-Bey, H., Zuo, W., Belin, P., Roussel, N., 2019. Weak bond strength between successive layers in extrusion-based additive manufacturing: measurement and physical origin. *Cement and Concrete Research*, 123, 105787.
- Marchment, T., Sanjayan, J. G., Nematollahi, B., Xia, M., 2019. Interlayer strength of 3d printed concrete: Influencing factors and method of enhancing. J. G. Sanjayan, A. Nazari, B. Nematollahi (eds), *3D Concrete Printing Technology*, Butterworth-Heinemann, 241–264.
- Mechtcherine, V., Bos, F. P., Perrot, A., Da Silva, W. L., Nerella, V. N., Fataei, S., Wolfs, R., Sonebi, M., Roussel, N., 2020. Extrusion-based additive manufacturing with cement-based materials – Production steps, processes, and their underlying physics: A review. *Cement and Concrete Research*, 132, 106037.
- Niemeier, W., 2008. *Ausgleichsrechnung: Statistische Auswertemethoden*. de Gruyter Lehrbuch, 2., überarb. und erw. edn, de Gruyter, Berlin.
- PERI GmbH, 2020a. 3D-Betondruck. <https://www.peri.com/de/geschaeftsfelder/3d-betondruck.html> (accessed 08 April 2021).
- PERI GmbH, 2020b. PERI builds the first 3D-printed residential building in Germany. <https://www.peri.de/informationsportal-news-medien/veroeffentlichungen-presse/peri-druckt-erstes-wohnhaus-deutschlands.html> (accessed 17 February 2022).
- Perkins, R., Gruev, V., 2010. Signal-to-noise analysis of Stokes parameters in division of focal plane polarimeters. *Optics express*, 18(25), 25815–25824.
- Sanjayan, J. G., Nematollahi, B., Xia, M., Marchment, T., 2018. Effect of surface moisture on inter-layer strength of 3D printed concrete. *Construction and Building Materials*, 172, 468–475.
- Snik, F., Craven-Jones, J., Escuti, M., Fineschi, S., Harrington, D., de Martino, A., Mawet, D., Riedi, J., Tyo, J. S., 2014. An overview of polarimetric sensing techniques and technology with applications to different research fields. D. B. Chenault, D. H. Goldstein (eds), *Polarization: Measurement, Analysis, and Remote Sensing XI*, SPIE Proceedings, SPIE, 90990B.
- Takruri, M., Abubakar, A., Alnaqbi, N., Shehhi, H. A., Jallad, A.-H. M., Bermak, A., 2020. DoFP-ML: A Machine Learning Approach to Food Quality Monitoring Using a DoFP Polarization Image Sensor. *IEEE Access*, 8, 150282–150290.
- Tipler, P. A., Mosca, G., Kersten, P. H., Wagner, J. H., 2019. *Physik*. 8. edn, Springer, Berlin, Heidelberg.
- Uno, P., 1998. Plastic Shrinkage Cracking and Evaporation Formulas. *Aci Materials Journal*, 365–375.
- Walsh, N. P., 2019. <https://www.archdaily.com/909534/worlds-largest-3d-printed-concrete-pedestrian-bridge-completed-in-china>, (accessed 17 February 2022).
- Wangler, T., Roussel, N., Bos, F. P., Salet, T. A., Flatt, R. J., 2019. Digital Concrete: A Review. *Cement and Concrete Research*, 123, 105780.
- Wolff, L. B., 1990. Polarization-based material classification from specular reflection. *IEEE Transactions on Pattern Analysis and Machine Intelligence*, 12(11), 1059–1071.
- Wolfs, R., Bos, F. P., Salet, T., 2018a. Correlation between destructive compression tests and non-destructive ultrasonic measurements on early age 3D printed concrete. *Construction and Building Materials*, 181, 447–454.
- Wolfs, R., Bos, F. P., Salet, T., 2019. Hardened properties of 3D printed concrete: The influence of process parameters on interlayer adhesion. *Cement and Concrete Research*, 119, 132–140.
- Wolfs, R. J. M., Bos, F. P., van Strien, E. C. F., Salet, T. A. M., 2018b. A real-time height measurement and feedback system for 3d concrete printing. D. A. Hordijk, M. Luković (eds), *High Tech Concrete: Where Technology and Engineering Meet*, Springer International Publishing, Cham, 2474–2483.
- Yamazaki, T., Maruyama, Y., Uesaka, Y., Nakamura, M., Matoba, Y., Terada, T., Komori, K., Ohba, Y., Arakawa, S., Hirasawa, Y., Kondo, Y., Murayama, J., Akiyama, K., Oike, Y., Sato, S., Ezaki, T., 2016. Four-directional pixel-wise polarization cmos image sensor using air-gap wire grid on 2.5-micrometres back-illuminated pixels. *2016 International Electron Devices Meeting*, IEEE, Piscataway, NJ, 8.7.1–8.7.4.
- Yingchuang Building Technique Co Ltd. (WinSun), 2022. <http://www.winsun3d.com/En/Product/prolist/id/1> (accessed 17 February 2022).